Research Open

Geology, Earth and Marine Sciences
Volume 7 Issue 6

Research Article

Boron in Some Variscan Deposits in the German Erzgebirge

Rainer Thomas*

Rainer Thomas, Im Waldwinkel 8, D-14662 Friesack, Germany

Corresponding author: Rainer Thomas, Im Waldwinkel 8, D-14662 Friesack, Germany

Received: August 29, 2025; **Accepted:** September 02, 2025; **Published:** September 05, 2025

Abstract

In this contribution, we show that boron can be found, beside in grey cast iron also in nature, transported via supercritical phases from mantle regions into the Earth's crust of the Variscan Erzgebirge/Germany. This boron is, as rule, contaminated by different boron compounds like boron carbide, boron nitride and others. We show further evidence that in supercritical phases transported or at low pressure formed diamond show most a large FWHM (>50 cm^{-1}), which is typically for this unusual diamond.

Keywords: *Boron, Boron Whisker, Diamond, Raman Spectroscopy, Variscan Erzgebirge*

Introduction

Boron is the fifth element of the periodic system and occurs in the Earth's crust only in its compounds (e.g., the simplest compound, boric acid [H_3BO_3] or more complex minerals as tourmaline, etc. In granite rocks, the average concentration of B is 15 ppm [1]. Boron is generally dependent on the content of impurities, mostly black. Thin boron crystals are transparent and orange- to yellow colored [2]. Boron has a very high affinity to carbon [3] and has, therefore, a bright black color. During the study of dissolution residues of the gray cast iron (Thomas et al., 2025), we found, besides diamonds, also nearby colorless boron in spheres or plate-like crystals. Table 1 shows the measured Raman data.

The Raman spectrum of boron from grey cast iron [4] is shown in Figure 1. E. Weintraub [7] first prepared pure elementary boron in 1909-1911 after a lot of misunderstanding by his predecessors [8,9]. According to Oganov (2010) [10], most of the discoveries related to pure boron were done in two "stages": 1957–1965 and 2001–2009. Boron does not exist in the Earth's high-oxygen environment. That is the state today. We will show that α- and β-Boron, together with boron oxides, carbides, and nitrides, can be found in Earth's material, which has significant importance and is the first observation ever. The rare appearance in different samples documents the strong reducing conditions of the supercritical fluid or melt [11-13]. Figure 2 shows a

Table 1: Measured important Raman lines of a-boron extracted from ductile cast iron [4,5] using the Raman line 532 nm, (the modes are according to Werheit et al., 2010 [3]).

α-Boron	[cm^{-1}]	Mode	n	Werheit et al. (2010) [cm^{-1}] [3]
First order	553.6		3	552
	575.2 ± 1.50	E_g	14	589
	591	E_g	1	589
	771.5	E_g	1	778
	795.4 ± 1.99	A_{1g}	11	795
	938.6	A_{1g}	1	934
	1096.2 ± 5.35		15	1094
Second order	1403.2		5	1409
	1583.6		3	1582
	1708.1		3	1710

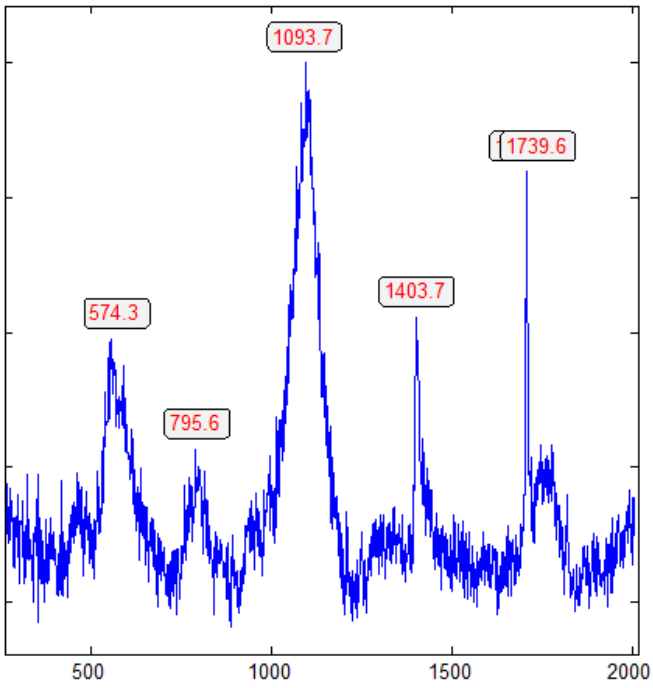

Figure 1: Raman spectrum of α-rhombohedral boron, contaminated by b-rhombohedral boron and boron carbide, shown by the strong and broad Raman band (A_{1g} + E_g) at 1093.7 cm^{-1}, typical for the b-rhombohedral boron [3] and the main peak of boron carbide around 1100 cm^{-1} [6].

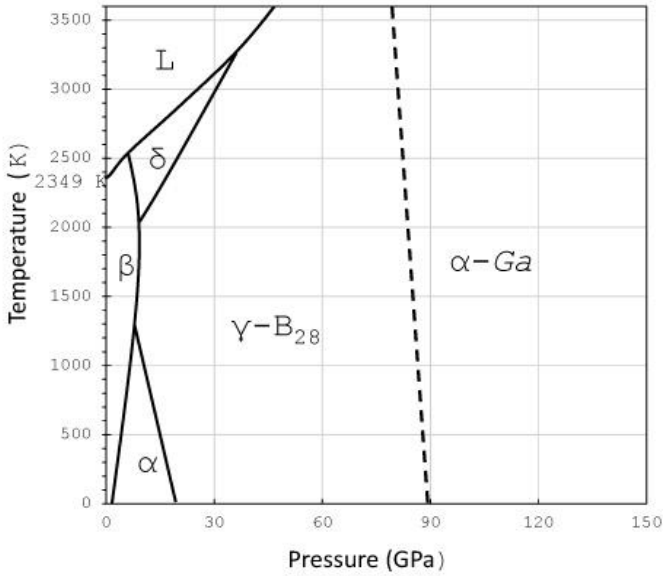

Figure 2: Schematic phase diagram of boron from Organov (2010) [10]. The γ-B_{28} and α-Ga types are special high-pressure phases, which are not crucial in our viewing and are not important here.a,b, and d stand for α–, β-, and δ-boron and L for liquid or molten boron.

schematic phase diagram of boron according to Organov (2010) [10], taken from Thomas et al. 2025b [5].

Besides diamond and boron, there are a couple of minerals (stishovite, coesite, cristobalite-X-I, orthorhombic cassiterite) in more crustal-formed as spherical minerals that demonstrate an interaction between the Earth's mantle and crust via supercritical fluid and/or melts. Because we find such minerals first and foremost in pegmatites and related mineralization, we will summarize here the data. Important are also the formation of boron and diamond whiskers in the crustal regions.

Natural Occurrence of Boron in the Upper Crust of the Variscan Erzgebirge

Boron in nature has not been found up to now. Only a lot of boron-bearing minerals are well known (e.g., boric acid, tourmaline, and many others). The formation of boron requires strong reducing conditions. Therefore, the occurrence of boron as smooth spherical inclusions in some minerals (cassiterite, quartz, topaz, fluorite, zinnwaldite) of the Variscan Erzgebirge is a surprising finding. Such spherical crystals occur in different minerals in Ehrenfriedersdorf, Sadisdorf, and Zinnwald. Of course, the boron is mainly a mixture of boron, boron carbide, and other minor phases, making the identification very difficult. In Figure 3, such an ellipsoid-shaped boron crystal in cassiterite from Ehrenfriedersdorf (Sn-58 Magdalena vein, second gangway (Mining Academy Freiberg, No. 11814) is shown.

The Raman spectrum is depicted in Figure 4. The main line at 478 cm^{-1} corresponds to $A_{1g} + E_g$ of β-rhombohedral boron; also, the bands at 630 (A_{1g}) and 773 cm^{-1}. The median strong band at 1106 cm^{-1} is, according to Werheit et al. (2010) [3], from β-rhombohedral boron with about 0.11 at% carbon. The 1082 cm^{-1} Raman band, according to Roma et al. (2022), is attributed to the boron carbide. The classification by the mixture of different β-phases according to Roma alone is not

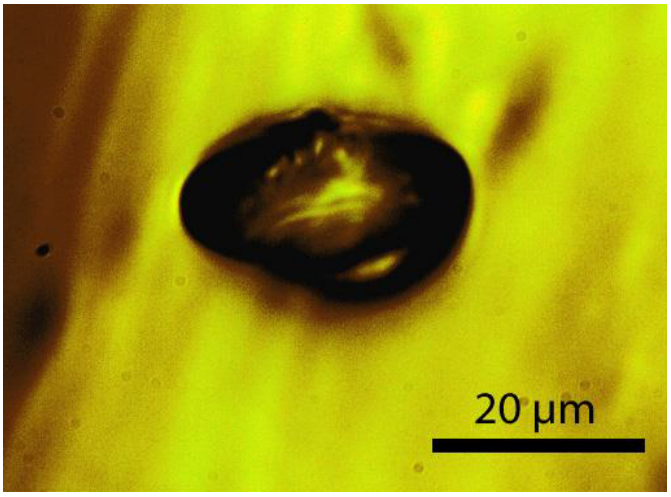

Figure 3: Spheroid of boron in cassiterite from Ehrenfriedersdorf (Sample: Sn-58). Well, to see their transparency.

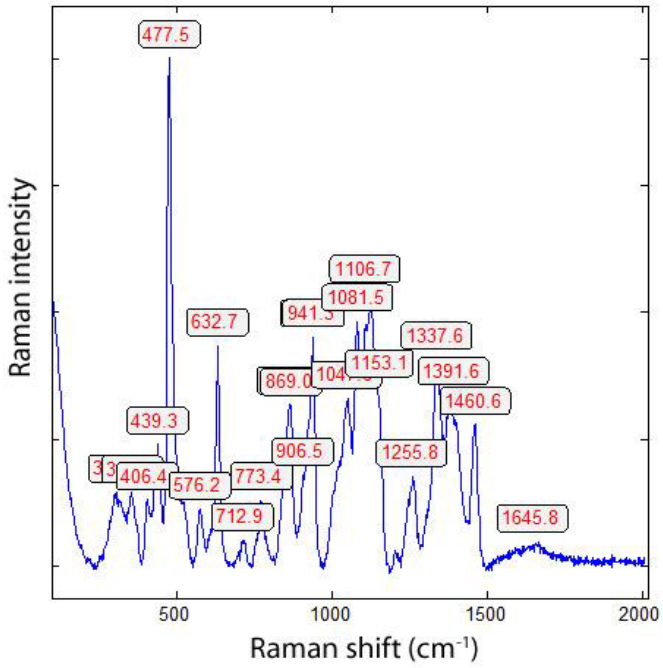

Figure 4: Raman spectrum of the boron crystal shown in Figure 3 (Sn-58). The strong lines 478 and 1106 cm^{-1} are from the β-rhombohedral boron [3]. The last one contains about 1.1 at. -% C.

possible, especially since traces of boron carbides and β-Si_3N_4can be present [14].

The measured Raman data are in Table 2 and are completed by some B compounds like BN, B_4C, and β-Si_3N_4 phases, which are not shown. The last phases are typical for boron from Zinnwald, especially in the mica mineral zinnwaldite.

The Raman spectrum from cassiterite Sn-58 shows signs of δ-boron. However, the line at 632.7 cm^{-1} is the main line of cassiterite, and the interpretation of this as a fingerprint line of the δ-boron is therefore doubtful. Difficulty is also the determination of δ-boron in quartz by the strong quartz line at 464 cm^{1}. Spherical boron inclusions in cassiterite (Sn-81 from Ehrenfriedersdorf) show the typical δ-boron

Table 2: Measured important Raman lines of a-, b-, and d-boron inclusion in cassiterite Sn-58 and Sn-81 using the Raman line 532 nm, (the modes are according to Werheit et al., 2010) as well as data for B-carbide and B-nitride from Roma et al., 2022, and Weringhaus, 1997, and Parakhonskoy, 2012.

α-Boron	**[cm^{-1}]**	**Mode**	**Werheit et al. (2010) [cm^{-1}] [3]**
First order	352.3	$A_{1g} + E_g$	357.0
	391.2		394.0
	576.2	E_g	575 ($B_{4.3}C$)
	591	E_g	589
	712.9	E_g	713
	773.4	E_g	774
	795.4 ± 1.99	A_{1g}	795
	869.0	E_g	873
	1081.5	A_{1g}	1094
Second order	1391.6		1409
	1460.6		1464
	1583.6		1582
	1708.1		1710
β-Boron			
	406.4		407
	477.5		480
	632.7	A_{1g}	627
	773.4		773
	1106.7	$A_{1g} + E_g$	1106 (0.1at.-% C)
δ-Boron	Sn-81 E-Dorf, 6th level		**Parakhonskoy (2012) [2]**
	360.2		361.0
	489.6		491.0
	629.2		631.0
	919.0		918.0
	1080.4		1078.0
Boron-carbide			**Roma et al. (2022)**
	319.2		320.0
	478.0		480.0
cBN			**Weringhaus (1997) [14]**
	941.3		950.7
	1016.9		1012.1
	1045.4		1045.6
	1045.4	TO (F_{2g})	1056.4
	1125.7		1123.1
	1337.6		1338.1
	1377.2	E_{2g}	1366.2

lines. According to Figure 2, the formation of δ-boron at about 30 GPa is quite possible and is typical for spherical inclusion in cassiterite brought by supercritical phases (Figure 5).

Typical for boron carbides [B_4C] are, according to Roma et al. (2022), the strong Raman bands at 319.2 and 478.0 cm^{-1}. Besides the spherical shape, there are also black whisker-like crystals in α-quartz from Zinnwald present (Figure 6). If the crystals are thin enough, the needles are transparent with a yellow shade. Often, we observe beside boron diamonds also as whiskers. The largest diamond crystal, beside a large boron crystal, has a diameter of 20 µm. In the α-quartz crystal, there are zones with hundreds of diamond and boron whiskers.

Figure 7 shows the spectrum of the boron needles as shown in Figure 6. There are also orthorhombic cross sections from boron present.

The α-quartz crystal from Zinnwald contains a lot of whisker or needle-like α-boron and diamond crystals (Figure 8), which include constant small amounts of β-boron. Particularly, the ends of those boron needles show a strong Raman band at 456 cm^{-1} (A_{1g} + E_g) characteristically for β-rhombohedral boron [3]. In Table 2 are the measured Raman bands of natural α- and β-boron summarized. Because the small needles are in quartz, the Raman measurements in

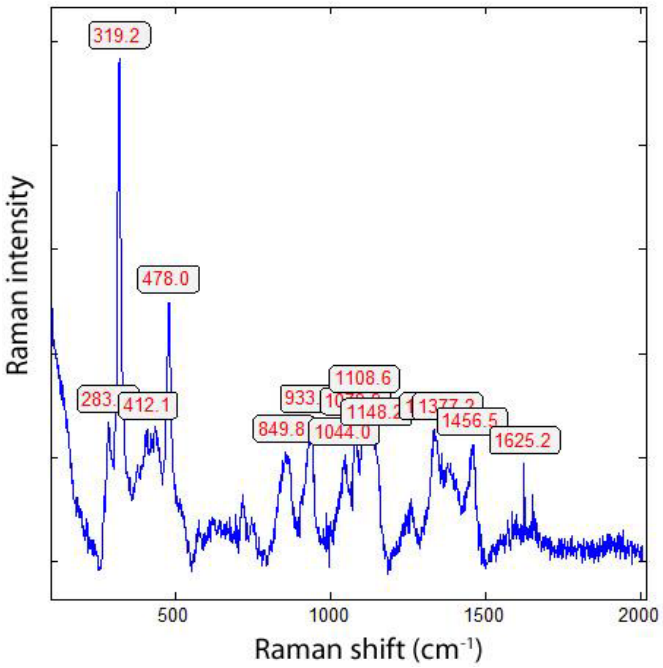

Figure 5: Raman spectrum of a mixture of boron and B_4C of a spherical crystal in zinnwaldite from Zinnwald/E-Erzgebirge.

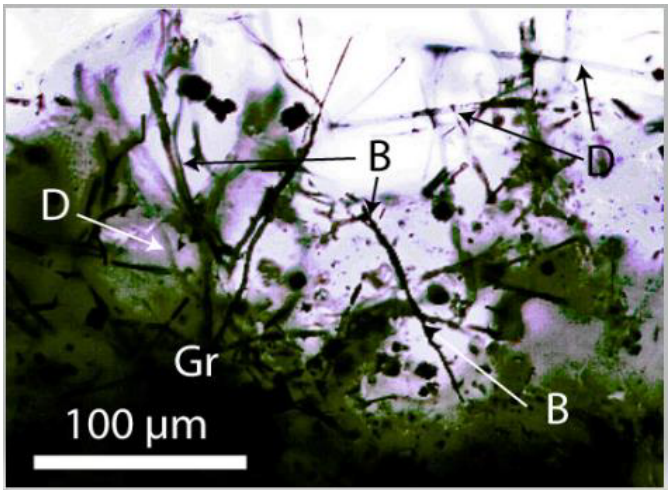

Figure 6: A mesh of diamond (D), bright boron (B) whiskers and graphite (Gr) in pegmatite quartz from Zinnwald/E-Erzgebirge.

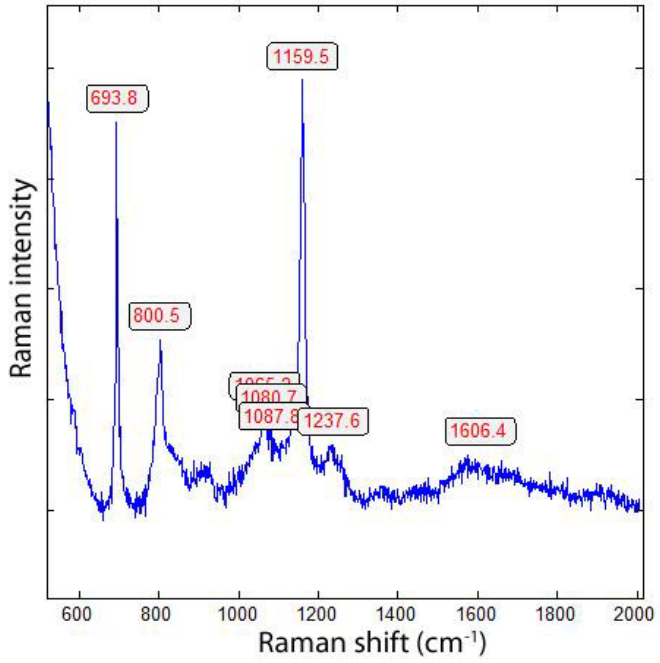

Figure 7: Raman spectrum of the boron needle in Figure 6. The bands at 694, 800, (1088), 1160, 2238 cm^{-1} are, according to Werheit et al. (2010) [3], typical for α-rhombohedral boron.

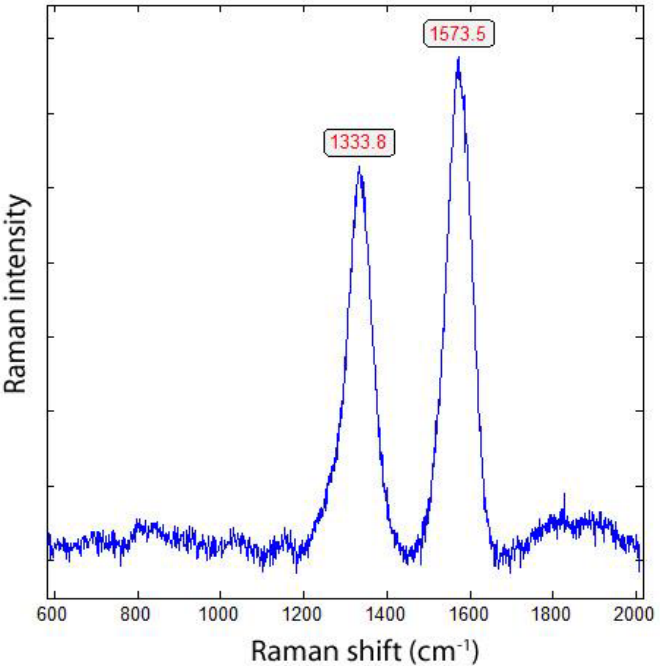

Figure 8: Typical Raman spectrum of a diamond whisker beside boron (see Figure 6) in quartz from Zinnwald/E-Erzgebirge. The FWHM are for the diamond line 69.8 and for the graphite line 72.8 cm^{-1}, respectively. FWHM – Full-Width at Half Maximum).

the low-frequency range are difficult due to the strong quartz bands in the low frequency range between 50 and 300 cm^{-1} and at 464 cm^{-1}). The tetragonal metastable δ- and ε-boron was not found up to now. Those remarks on boron should be enough to show the strong reducing conditions during the interaction of supercritical fluids with the Variscan mineralization. If we use the pressure-temperature diagram for SiO_2 polymorphs from Frondel (1962) [15] and use the results from Zinnwald quartz [16], the coexistence of α-quartz with coesite and boron results in a more or less exact temperature value of 1300°C and a pressure of nearly 3.4 GPa, corresponding to about the triple point of high-quartz, low-quartz, and coesite. The triple point of α-boron, β-boron, and γ-B_{28} boron is very near the called SiO_2 triple point [14]. Such values are realistic for supercritical fluid if they meet the crustal granitic rocks. However, these values are too low according to the experimentally determined equilibrium curve for diamond-graphite [17]. Figure 8 is a typical Raman spectrum of a diamond whisker in quartz from Zinnwald.

In a couple of works [4,5,16,18,19], we have shown many diamond crystals formed at low pressure (in grey cast iron or in nature) or transported into a high crusal level via supercritical fluids or melt. All such diamonds typically have a large FWHM. According to Ferrari and Robertson (2004) [20], the incredible versatility of carbon is explained by the strong dependence of its physical properties on the ratio of sp^2 (graphite-like carbon) to sp^3 (diamond-like carbon). They show this in their ternary phase diagram (Figure 1 in this). A mostly dark color characterizes the diamonds formed or deposited at low pressure (technical processes, nature). Also, the boron crystals are mostly very dark due to contamination. The boron whiskers in the Zinnwald quartz are typical bright black. In this contribution, we have restricted ourselves to examples from the Variscan mineralisations in the German Erzgebirge. However, we know that in a lot of other pegmatites and granites, boron and diamonds, and similar HP and HT minerals are present.

Discussion

We have found, as mineral inclusions of the Variscan Erzgebirge, a lot of high-pressure and high-temperature minerals like beryl-II, α-, β- and δ-boron, boron carbide, diamond, coesite, cristobalite X-I, graphite, silicon carbide, stishovite, as well as gas phases CH_4, H_2 and D_2 at high density [21-23]. That means at least that the supercritical fluids and melts will feed a large amount of water into the crust coming from the mantle regions. The high velocity of the supercritical fluids also brings primarily smooth spherical crystals. The supercritical fluids/melt have a large amount of energy, which can, at the transition to the under critical stage, make the necessary room for pegmatites and vein mineralizations and also bring a large amount of ore-forming elements with it. That means at least a lot of observations in the past are of secondary meaning. At that place, the extreme element enrichment according to Lorentzian-like curves as proof of the meaning of supercritical fluids is foregone, because we have discussed this point enough [24]. Because elemental boron in an oxidized surrounding and high temperatures is not stable, it must form more stable compounds, like boric acid and many other B-bearing minerals. Another critical point is that a large part of boron comes directly from the mantle region and not from the Earth's surface, as is often assumed.

Appendix: Microscopy and Raman Spectroscopy of Boron-rich Phases in Variscan Minerals of the Erzgebirge

Besides a polarization microscope for transmission and reflection (JenaLab Pol), we performed all microscopic and Raman spectroscopic

studies with a petrographic polarization microscope (BX 43) with a rotating stage coupled with the EnSpectr Raman spectrometer R532 (Enhanced Spectrometry, Inc., Mountain View, CA, USA) in reflection and transmission. The Raman spectra were recorded in the spectral range of 0–4000 cm^{-1} using an up to 50 mW single-mode 532 nm laser, an entrance aperture of 20 µm, a holographic grating of 1800 g/mm, and a spectral resolution of 4 cm^{-1}. Detailed descriptions of the methods used are given by Thomas et al. (2025a and 2025b) [4,5]. For the identification of mineral phase, we used Hurai et al. (2015) [25] and the RRUFF database by Lafuente et al. (2015) [26,27]. From our studies [5], we found that the measuring spot at the sample using the high-quality 100x objective is ~1µm. From this, a high energy density results. To prevent intense heating during the measurement and formation of sp^2 carbon in diamond, we used 4 mW on the sample and, for fast routine measurements, 30 mW.

Acknowledgment

Thanks go to many colleagues who inspired this Raman work on high-pressure and temperature minerals in the Earth's crust.

References

1. Rösler HI, Lange H (1975) Geochemische Tabellen. Leipzig. Pg: 675.
2. Parakhonskiy G (2012) Synthesis and investigation of boron phases at high pressure and temperatures. Dissertation at the University of Bayreuth. Pg: 117.
3. Werheit H, Filipov V, Kuhlmann U, Schwarz U, Armbrüster M, et al. (2010) Raman effect in icosahedral boron-rich solids. *Science and Technology of Advanced Materials*. 11.
4. Thomas R, Brümmer G, Scheiblauer K (2025a) Unexpected carbon phases in grey cast iron – diamond, calcite, and methane. *Geology, Earth and Marine Sciences*. 7: 1-6.
5. Thomas R, Brümmer G, Scheibblauer K (2025b) Paradigm change of pegmatite formation – where does the water come from?. *Geology, Earth and Marine Sciences*. 7: 1-7.
6. Roma G, Gilles K, Jay A, Vast N, Gutierrez G (2021) Understanding first order Raman spectra of boron carbides across the whole stochiometry range. Physical *Review Materials*. 5: 1-31.
7. Weintraub E (1911). On the properties and preparation of the element boron. *J. Ind. Eng. Chem.* 3: 299-301.
8. Meyer RJ (1926) Gmelins Handbuch der Anorganischen Chemie – Bor. Verlag CChemie, Leipzig-Berlin. Pg: 142.
9. Pietsch EHE (1954) Gmelins Handbuch der Anorganischen Chemie – Bor. Weinheim. Pg: 253.
10. Organov AR (2010) Boron under pressure: Phase diagram and novel high-pressure phase. NATO Science for Peace and Security Series B: Physics and Biophysics – Boron rich solids. (Eds) By Orlovskaya N and Lugovy M. *Springer*. Pg: 207-225.
11. Ni H (2023) Introduction to advances in the study of supercritical geofluids. Science China: Earth Science. 66: 2391-2394.
12. Ni H, Zhang L, Xiong X, Mao Z, Wang J (2017) Supercritical fluids at subduction zones: Evidence, formation condition, and physicochemical properties. *Earth-Science Reviews*. 167: 62-71.
13. Sun Y, Liu X, Lu X (2021) Structures and transport properties of supercritical SiO_2-H_2O and $NaAlSi_3O_8$-H2O fluids. *American Mineralogist*. 108: 1871-1880.
14. Werninghaus T (1997) MicroRaman spectroscopy investigations of hard coatings. Dissertation, TU Chemnitz-Zwickau. Pg: 163.
15. Frondel C (1962) The System of Mineralogy. Volume III, Silicate Minerals. John Wiley and Sons, INC. Pg: 334.
16. Thomas R (2025) Diamond, diamond whisker, graphite, carbon, and coesite in a quartz crystal from Zinnwald, E-Erzgebirge. *Geology, Earth and Marine Sciences*. 7: 1-6.
17. Day HW (2012) A revised diamond-graphite transition curve. *Am. Mineralogist*. 97: 52-62.
18. Thomas R (2023) Diamond in pegmatitic sillimanite from Reinbolt Hills/East Antarctica. *Geology, Earth and Marine Sciences*. 5: 1-3.
19. Thomas R (2024) ^{13}C-rich diamond in a pegmatite from Rønne, Bornholm Island: Proofs for the interaction between mantle and crust (2024*). Geology, Earth and Marine Sciences*. 6: 1-3.
20. Ferrari AC, Robertson J (2004) Raman spectroscopy of amorphous, nanostructured, diamond-like carbon, and nanodiamond. *Phil. Trans. R. Soc. Lond.* 362: 2477-2512.
21. Thomas R, Webster JD (2000) Strong tin enrichment in a pegmatite-forming melt. *Mineralium Deposita*. 3: 570-582.
22. Thomas R, Davidson P, Rericha A, Voznyak DK (2022b) Water-rich melt inclusions as "frozen" samples of the supercritical state in granites and pegmatites reveal extreme element enrichment resulting under non-equilibrium conditions. *Mineralogical journal (Ukraine)*. 44: 3-15.
23. Thomas R, Davidson P, Rericha A, Recknagel U (2023) Ultrahigh-pressure mineral inclusions in a crustal granite: Evidence for a novel transcrustal transport mechanism. *Geosciences*. 13: 1-13.
24. Thomas R, Rericha A (2024) Extreme element enrichment, according to the Lorentzian distribution at the transition of supercritical to critical and under-critical melt or fluids. *Geology, Earth and Marine Sciences*. 6: 1-6.
25. Hurai V, Huraiova M, Slobodnik M, Thomas R (2015) Geofluids – Developments in Microtermometry, Spectroscopy, Thermodynamics, and Stable Isotopes. *Elsevier*. Pg: 489.
26. Lafuente B, Downs RT, Yang H, Stone N (2016) The power of database: The RRUFF project. In: Highlights in MineralogicalCrystallography, Armbruster T, Danisi RM (Eds) De Gruyter: Berlin, München, Boston. Pg: 1-30.
27. Thomas R, Trinkler M (2024) Monocrystalline lonsdaleite in REE-rich fluorite from Sadisdorf and Zinnwald/E-Erzgebirge, Germany. *Geology, Earth and Marine Sciences*. 6: 1-5.

Citation:

Thomas R (2025) Boron in Some Variscan Deposits in the German Erzgebirge. *Geol Earth Mar Sci* Volume 7(6): 1-5.